Project No. 09-843

Microscale Heat Conduction Models and Doppler Feedback

Reactor Concepts

Dr. Ayman I. Hawari
North Carolina State University

In collaboration with:
Idaho National Laboratory

Madeline Feltus, Federal POC
Abderrafi Ougouag, Technical POC

NEUP Nuclear Energy University Programs
U.S. Department of Energy

FINAL TECHNICAL REPORT

Project Title: MICROSCALE HEAT CONDUCTION MODELS AND DOPPLER FEEDBACK

Covering Period: October 1st, 2009 through September 30th, 2012

Date of Report: January 7, 2015

Recipient: North Carolina State University
P.O. Box 7909
Department of Nuclear Engineering
Raleigh, NC 27695-7909

Project Number: 09-843

Principal Investigator: Ayman I. Hawari
(919) 515-4598
ayman.hawari@ncsu.edu

Collaborators: Abderrafi Ougouag
Abderrafi.Ougouag@inl.gov

Project Objective: The objective of this project is to establish an approach for providing the fundamental input that is needed to estimate the magnitude and time-dependence of the Doppler feedback mechanism in Very High Temperature reactors. This mechanism is the foremost contributor to the passive safety of gas-cooled, graphite-moderated high temperature reactors that use fuel based on Tristructural-Isotropic (TRISO) coated particles. Therefore, its correct prediction is essential to the conduct of safety analyses for these reactors. Since the effect is directly dependent on the actual temperature reached by the fuel during transients, the underlying phenomena of heat deposition, heat transfer and temperature rise must be correctly predicted. To achieve the above objective, this project will explore an approach that accounts for lattice effects as well as local temperature variations and the correct definition of temperature and related local effects.

Background: Most High Temperature Gas Reactor (HTGR) codes only include a homogenized pebble or compact shell model, which approximates the temperature of the fuel region. However, in these reactors the fuel region includes the TRISO particles and the surrounding graphite matrix, therefore the fuel temperature prediction is not always well represented. These models produce reasonable results for steady state and very slow

transient conditions. For fast transients, an explicit model is necessary in order to predict accurately the fuel temperature. The main unresolved issue with the current model pertains to two facts. The first is that the establishment of temperature following the fission event is not well defined. The second, and possibly the most important, is that the energy deposition in the fuel kernel is not uniform; on the contrary, it is very much a localized phenomenon where 90-95% is transferred to electrons. As the electrons slow down, electron-phonon interactions are initiated. Finally, this translates into lattice heat transfer (i.e., into atomic lattice vibrations). This description of the events that take place at the microscopic level renders the assumption of constant energy deposition across the fuel kernel unusable for small time scales. This effect (and possible secondary ones) will likely result in a variable magnitude of the Doppler effect within a TRISO fuel kernel. The consequence of this variation stems from the non-linearity of the temperature dependence on the amount of deposited energy (i.e., the temperature dependence of the heat capacity) and the non-linearity of the Doppler effect proper, as the temperature appears as an exponential term in the expression of the resonances. These physical considerations suggest that a given amount of energy distributed into local pockets within the TRISO kernel may impact the Doppler effect differently than the same amount uniformly distributed over the entire kernel.

Status: Uranium dioxide (UO_2) is the most widely used fuel material for nuclear power reactors; its atomic and electronic structures are shown in figures 1 and 2. Upon exposure to neutrons, the uranium nuclei can fission resulting in the release of over 200 MeV of energy and the deposition of 170 MeV of energy directly in the fuel. The fission process and its immediate consequences (including the creation of energetic heavy fission fragments) can highly impact the fuel's atomic lattice.

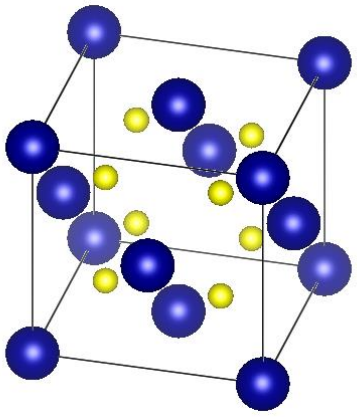

FIG. 1. Uranium dioxide crystallizes into a fluorite structure (space group F-m-3m). Uranium atoms are blue (dark) and oxygen atoms are yellow (light).

In this project, the impact of electronic structure on fission energy deposition in UO_2 is examined using classical molecular dynamics simulations and by invoking the two temperature model (TTM) to describe the interaction between the electronic structure and the lattice. Table 1 gives the correlation between electronic structure and the thermal conductivity for various fuel and other materials.

Table 1. Correlation of electronic structure to thermal conductivity. For UO_2 and ZrO_2 the size of the band gap (E_g) is given.

Material	Material Type	κ [W/m/K][18-21]
UN	Metal	24
UC	Metal	20
UO_2	Insulator (E_g = 2eV)[10]	3
ZrO_2	Insulator (E_g = 6eV)[22]	2

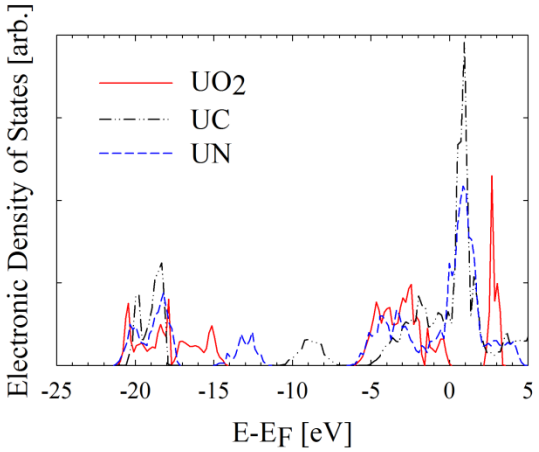

FIG. 2. Electronic structure of several nuclear fuel materials (UN, UC, and UO_2) as obtained in this work through DFT calculations using the VASP code with the Perdew-Burke-Ernzerhof pseudopotentials, a generalized-gradient approximation for the exchange correlation, and the addition of a Hubbard model for UO_2. The energy is referenced to the Fermi level, E_F, the highest occupied energy level at zero kelvin. For UC and UN the availability of states is continuous across the Fermi level, where as in UO_2 a 2eV band gap is observed.

Fission represents the initiating and driving event for the phenomenon examined in this work. The fission process results in the production of two fission fragments with a total kinetic energy of approximately 170 MeV. High temperature fission spikes are caused by the deposition of

fission fragment energy within the fuel matrix. The initial deposition of energy in a material by fission fragments can be expressed by the stopping power,

$$(-dE/dx)_t = (-dE/dx)_e + (-dE/dx)_n + (-dE/dx)_r , \quad (1)$$

where $(-dE/dx)_t$ is the total energy loss per unit path length, $(-dE/dx)_e$ is the loss due to interactions between the fission fragment and electronic structure, $(-dE/dx)_n$ is the loss due to collisions with atomic nuclei, and $(-dE/dx)_r$ is the radiative loss. Radiative losses are a relativistic effect and are negligible for fission fragments. Typical fission fragments have stopping powers of 18 keV/nm (100 MeV) and 22 keV/nm (70 MeV) for light fission fragments (LFF) and heavy fission fragments (HFF) respectively. The relative contributions of the electronic and collisional components of stopping power for such typical LFF and HFF was determined using SRIM code calculations. As it can be seen in Fig. 3, the electronic stopping power is the dominate mechanism of energy loss at high energies, and is also dominant along most of the fission fragment path. As a result of the fission event and the energy deposition by the LFF and HFF, temperature and pressure spikes develop in the atomic lattice resulting in what is known as the “fission spike”. The observed dominance of electronic stopping along the path of a fission fragment implies that the primary component of a fission spike originates in the electronic structure. Consequently, simulating the fission spike and observing the evolution of its impact in a UO_2 system following a fission event would be a reasonable starting point for the investigation of fission driven phenomena.

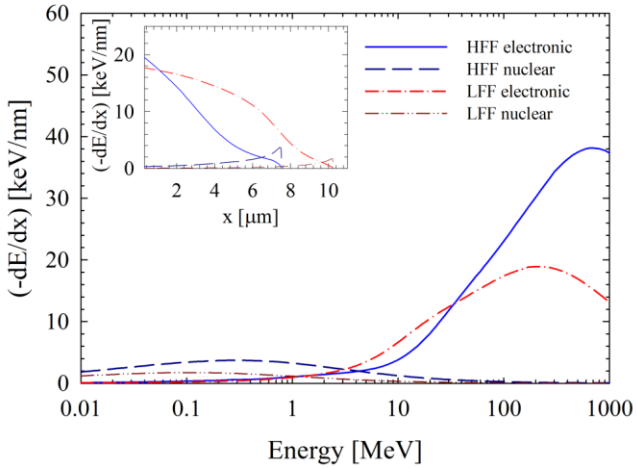

FIG. 3. Electronic and nuclear stopping power of typical fission fragments calculated with the SRIM code.

A common model used to describe fission spikes in materials is the two temperature model (TTM). This model attempts to capture the energy exchange between the electronic and lattice systems through electron-phonon scattering while explicitly treating energy transport within the electronic system, and may be used to describe the evolution of a fission spike with energy originating in the electronic system. This model has been demonstrated to be a reasonable predictive tool in exploring the evolution of electronic excitations in atomic systems, and is used in this work to describe fission-lattice interaction. The model is described by the heat equations

$$\rho_e C_e \partial T_e / \partial t = \nabla (k_e \nabla T_e) - g_{ep}(T_e - T_a) + B(\mathbf{r},t) + g_s T'_a \quad \textbf{(2)}$$

$$\rho C(T_a) \partial T_a / \partial t = \nabla (k(T_a) \nabla T_a) + g_{ep}(T_e - T_a) - g_s T'_a \quad \textbf{(3)}$$

where T_e, T_a, ρ, ρ_e, C_e, $C(T_a)$, and k_e, $k(T_a)$ are the temperature, particle number densities, specific heat, and thermal conductivities of the electronic and lattice system, respectively. The additional terms describe the initial energy injection into the electronic system, $B(\mathbf{r},t)$, and the energy exchange between the electron and lattice systems through electron-phonon coupling, g_{ep}, and electronic stopping, g_s. In the intial stages of a fission spike, atoms may exceed a threshold velocity, corresponding to a temperature of T'_a, and suffer electronic energy loss described by an electronic stopping coupling factor, g_s. The initial energy injection into the electronic system, $B(\mathbf{r},t)$, which is representative of the delta-ray dose resulting from a fission fragment, or other swift heavy ion, may be represented by an exponential function,

$$B(\mathbf{r},t) = (-dE/dx)_e \pi N \exp(-r/R) \exp(-t/t_f), \quad \textbf{(4)}$$

where $(-dE/dx)_e$ is the electronic stopping power, and N is a normalization constant. The mean radius of delta-ray energy deposition, R, is dependent on the energy (MeV/amu) of an incident ion and may be estimated to be between 1-4 nm in UO_2 for heavy ions of interest. Delta rays slow down through electron scattering interactions and excite secondary electrons within a mean time of flight, t_f, of approximately 5 femtoseconds (fs). Subsequently, these excitations quickly thermalize through electron-phonon inelastic scattering within 10-1000 fs, transferring energy to the atomic lattice. This inelastic scattering process is described by the electron-phonon coupling constant g_{ep}, a parameter related to the electron-phonon scattering cross-section. The energy exchange rate between electronic excitations and the atomic lattice may be described with the cross-section formalism,

$$g_{ep}\Delta T = (4\pi/\hbar)\sum_{k,k'} E_q \left|M_{k,k'}\right|^2 S(k,k')\delta(E - E_{k'} + E_q) \quad \textbf{(5)}$$

where ΔT is the temperature difference between electronic excitations and the local atomic lattice, and k and q are the electron and phonon momentum respectively. The scattering matrix $M_{k,k'}$ defines the probability of electrons scattering from state k to k'. The scattering of an electron from energy E_k to energy $E_{k'}$ occurs by the emission or absorption of a phonon of energy E_q; a process described by $S(k,k')$. Equation (5) shows that transition rate, the pre-cursor to the scattering cross-section, of e-p interactions is correlated to a characteristic time between scattering events defined by the electron-phonon coupling time, τ_{ep}. Within the free electron gas approximation, the electron-phonon coupling constant may be estimated in terms of an electron-phonon coupling time as

$$g_{ep} = \rho_e C_e / \tau_{ep} \,. \quad \textbf{(6)}$$

A free electron gas has an electronic heat capacity of $3/2k_B$, where k_B is Boltzmann's constant. The specific heat, i.e. the product of density and heat capacity may be assumed to be characteristic of a noble metal with a value of approximately 10^6 $J{\cdot}m^{-3}{\cdot}K^{-1}$. The electronic thermal conductivity, a description of energy transport, varies directly with the characteristic time between any electron scattering events. The dynamics of scattering in a non-equilibrium disruption resulting from fission is not well established, so in this work both the thermal conductivity and electron-phonon coupling time were treated as adjustable parameters. A free electron gas in a metal is estimated to have a thermal conductivity and electron phonon coupling time of approximately 200 $W{\cdot}m^{-1}{\cdot}K^{-1}$ and 1000 fs respectively. Therefore, decreasing electron-phonon coupling times and thermal conductivity are indicators of increasing insulator character. For UO_2, a Mott-Hubbard insulator, a thermal conductivity of nearly 20 $W{\cdot}m^{-1}{\cdot}K^{-1}$ and an electron-phonon coupling constant within the range of 100-300 fs were used in the simulation of heavy ion spike evolution. The transfer of energy to the atomic lattice by electron-phonon coupling results in the development of a thermal spike composed of a central melted core surrounded by a heated zone; a phenomenon which is expected to be enhanced in insulators in comparison to metals.

Classical molecular dynamics (MD) was used in this work to explore e-p coupling and its consequences in UO_2. The interactions between atoms were described by a Coulomb-Buckingham interatomic potential,

$$V_{ij} = A_{ij} \exp(-r/\rho_{ij}) - C_{ij}/r_{ij}^6 - (1/4\pi\varepsilon_0)(Z_i Z_j / r_{ij}) \quad (7)$$

The potential parameters were tuned to provide reasonable agreement with lattice expansion, bulk modulus, and thermal conductivity. The MD simulations in this work were performed on a GPU cluster using the LAMMPS code, which utilizes the particle-particle particle-mesh (PPPM) method for treating the long-ranged coulomb interactions between atoms. Fission spikes resulting from electronic stopping were modeled in a 10x60x60 super-cell, 432000 atoms, representing a cross-section perpendicular to fission fragment trajectory. Prior to the simulation of a fission spike, the super-cell was relaxed under an NVE thermostat (i.e. micro-canonical ensemble) with a Langevin bath outside of a cylinder with a radius of 28 unit-cell lengths. This bath was also used in simulations of fission spikes, and was found to be sufficiently large to capture the thermal spike phenomena.

In the current MD-TTM simulations of fission spikes and ion spikes, the electronic subsystem was treated using the continuum model formulated in Eq. (2), and used a stochastic force to capture the energy exchange between the atomic and electronic subsystems. The electronic subsystem was composed of 10x60x60 finite element cells and contained a bath with the same temperature and dimensions as that for the atomic lattice. To capture the changing time scales of the phenomenological development of fission and ion spikes, the time steps were varied from 10 attoseconds (as) at the initial injection of electronic energy to 1 fs during the quenching of the resulting thermal spike.

The phenomenological evolution of a fission spike, simulated using MD-TTM, is illustrated in Fig. 4. The corresponding changes in uranium density due to a fission spike are shown in Fig. 5. The density was calculated within 1 nm thick shells around the initial fission spike center. At approximately 20 ps the fission spike has subsided, and the relative density outside a radius of approximately 3nm has been restored to the initial level. However, as expected in a fission track, the vacancy rich zone developed during the quenching phase does not fully anneal, resulting in a vacancy rich core within the track. The high density zone encompassing the vacancy rich zone is the interstitial zone; however, the density increase may be partially explained by residual stress within the track.

Latent ion tracks are structural disruptions that may be observed visually in MD simulation, as demonstrated in Fig. 6; however, quantitative estimation of an ion track size is also accessible in MD. Pair-

correlation functions measure the atomic structure of a system, and were used in this work to determine the size of a track. Estimates of the pair-correlations within 0.5 nm thick cylindrical shells centered about simulated fission fragment or heavy ion trajectory demonstrated either disordered or structured character corresponding to track or non-track behavior respectively. A transition region exists between the amorphous and structured zones in which some structure has re-emerged but the lattice is not yet completely distinguishable. The track radius was defined to be the mean radius within this transition region. The transition between track and structured regions after the annealing phase of a 29 keV/nm thermal spike in an insulator-like system at 300 K with a 150 fs electron-phonon coupling time and thermal conductivity of 20 $W \cdot m^{-1} \cdot K^{-1}$ is shown in Fig. 7.

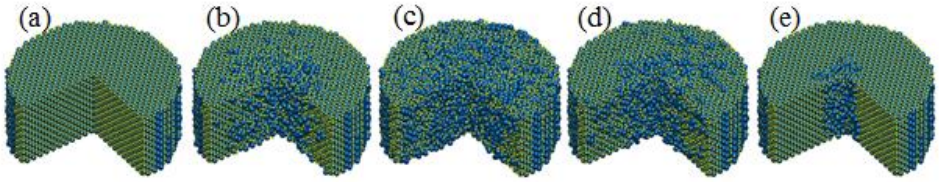

FIG. 4. Evolution of 29 keV/nm thermal spike in a simulated insulator-like system with τ_{ep} of 150 fs. The fission spike time progression from left to right is (a) original crystal, (b) ballistic phase, (c) quenching phase, (d) annealing phase, and (e) latent track. Uranium atoms are blue (dark) and oxygen atoms are yellow (light).

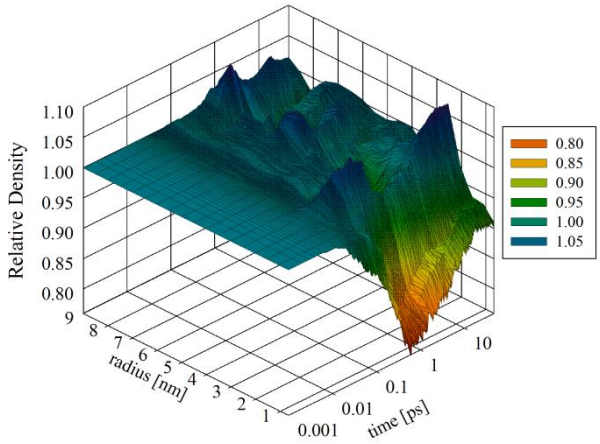

FIG. 5. Evolution of relative uranium density resulting from a 29 keV/nm thermal spike in a simulated insulator-like system with τ_{ep} of 150 fs. The relative density is referenced to the initial density within each zone.

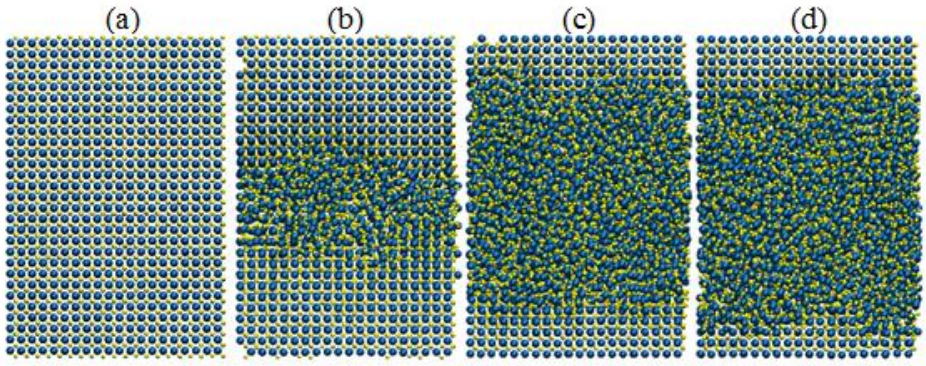

FIG. 6. (a) Pristine crystal and latent tracks resulting from (b) 29 keV/nm, (c) 56 keV/nm and (d) 59 keV/nm thermal spike in an insulator-like system with τ_{ep} of 150 fs. Uranium atoms are blue (dark) and oxygen atoms are yellow (light).

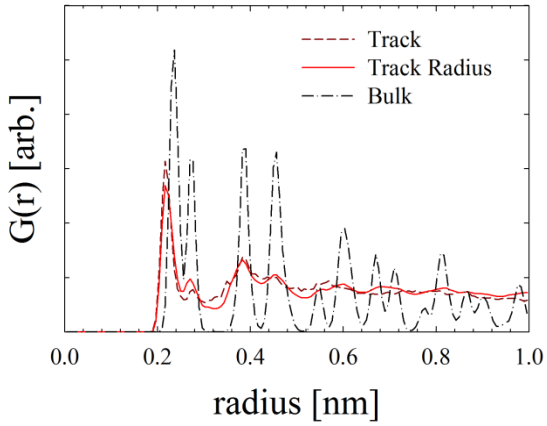

FIG. 7. Pair-correlation function, G(r), for a simulated 29 keV/nm ion track in a system with a τ_{ep} of 150 fs and k_e of 20 $W \cdot m^{-1} \cdot K^{-1}$. The pair correlation functions were measured within 0.5 nm thick cylindrical zones centered about the simulated particle trajectory.

As discussed above, the evolution of a fission spike leading to a track may be characterized by a thermal spike in which the lattice temperature spikes due to the rapid deposition of electronic energy to the lattice system and subsequently decays by phonon transport. The sudden expansion of the hot inner core of the fission spike may result in a pressure spike in addition to the temperature spike. The temperature and associated pressure spike, as demonstrated in Figs. 8-10, are expected to become more pronounced with decreasing electron-phonon coupling time. Increasing metallic behavior, i.e. weaker e-p coupling, and decreasing electronic stopping power are observed to result in a less

pronounced thermal spike and associated pressure spike. Latent tracks, as indicated in Fig. 8b, or oxygen defect clusters in the case of fission fragments, are observed to possess residual stress energy which exert pressure on the surrounding bulk crystal.

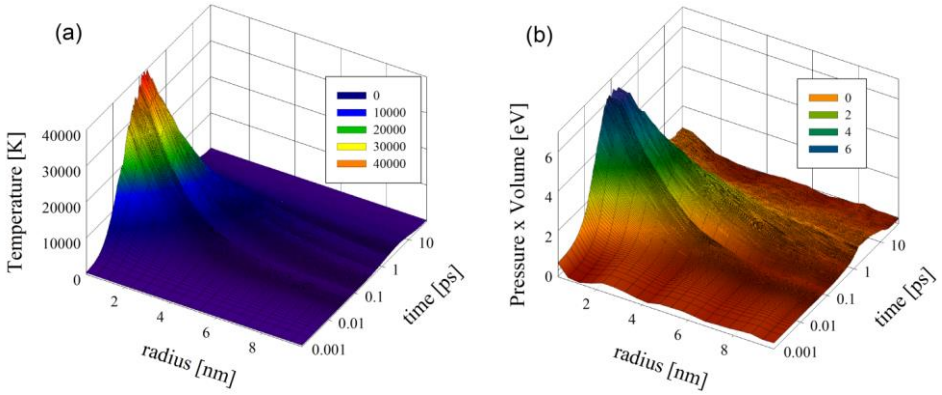

FIG. 8. (a) Temperature and (b) pressure spikes for a simulated 29 keV/nm ion in an UO_2 system with τ_{ep} of 150 fs. The temperature distributions illustrate the rapid increase in lattice energy in a thermal spike followed by a slower quenching of heat from a molten zone. The pressure spikes are shown as stress energy, pressure × volume, illustrating the development and decay of a pressure gradient. A stress zone may be observed around the latent track, which has a radius of 1.2 nm.

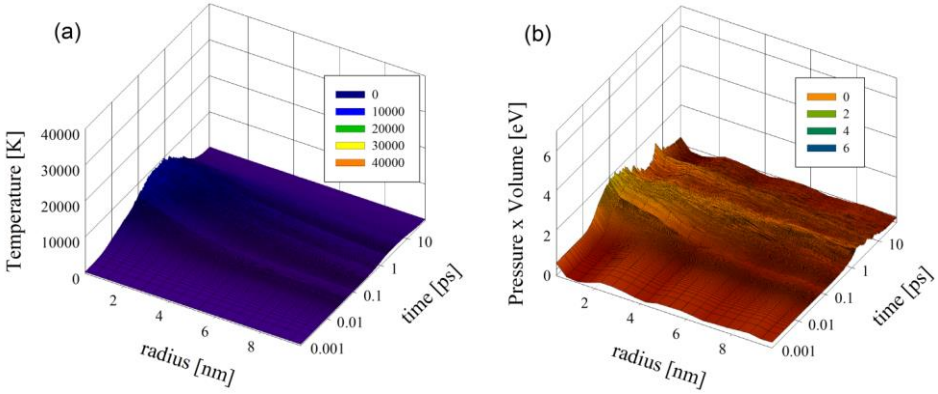

FIG. 9. (a) Temperature and (b) pressure spikes for a simulated 29 keV/nm ion in an UO_2 system with τ_{ep} of 1000 fs.

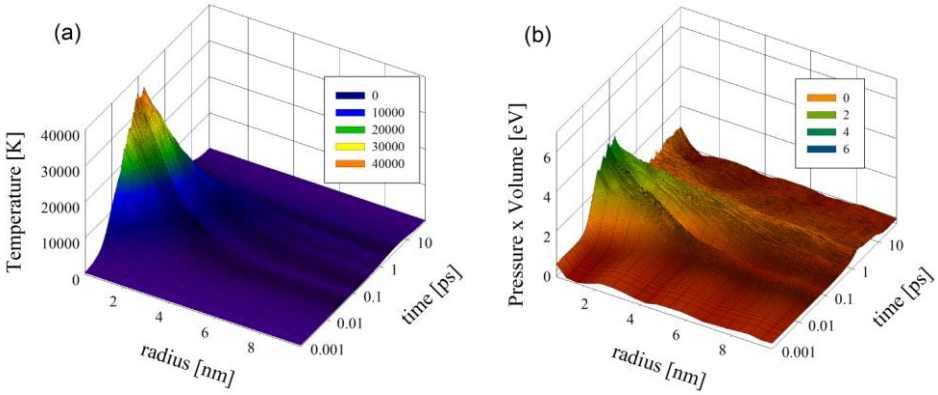

FIG. 10. (a) Temperature and (b) pressure spikes for a simulated 22 keV/nm fission fragment in an UO_2 system with τ_{ep} of 150 fs. While no track was observed for fission fragments, a stress zone from oxygen defect clusters may be observed near the simulated fission fragment path.

The track radii predicted by MD-TTM for a range of stopping powers and for various electron-phonon coupling times are compared to experiment in Table II. The existence of each track was verified by visual observation of the MD super-cell following the simulated irradiation. Variation in the electron-phonon coupling time demonstrates that increasing coupling strength results in larger track radius. The track radii predicted for ions of the same stopping power have reasonable agreement with experiment within the previously determined range of electron-phonon coupling times. Specifically, a coupling time of 150 fs has reasonable agreement with predicted track radii and is within reasonable proximity to the predicted value of 180 fs for UO_2 based on a correlation between coupling and band gap.

Table I. Track Radius for various electronic stopping powers and electron-phonon coupling times. The MD-TTM electronic system had a 20 $W \cdot m^{-1} \cdot K^{-1}$ for all τ_{ep}. The experimental data are 173 MeV (29 keV/nm) Xe ions, 1300 MeV (56 keV/nm) uranium ions, and 2713 MeV (59keV/nm) uranium ions in UO_2.

S_e [keV/nm]	Track Radius [nm]				
	Electron-phonon Coupling time [fs]				Exp[9]
	1000	300	200	150	
18	0	0	0	0	0
22	0	0	0	0	0
29	0	0	1.0	1.2	1.7±0.2
56	0	2.3	2.7	3.1	4.4±0.5
59	0	2.5	3.0	3.3	4.8±0.5

The above results establish a verfified computational approach for generating the input needed to assess the impact of localized heated zones (e.g., due to a fission event) on phenomena such as the Doppler effect in a nuclear reactor.

In addition, in this work, modification to the NJOY code were made to implement a formulation similar to Borgonovi's based on the use of the dynamic structure factor for assessing the Doppler broadening of neutron absorption resonances was implemented. The neutron absorption resonance may be described by the Breit-Wigner resonance. The line shape of this resonance including the effects of the thermal motion of the target is described by

$$W(E) = \frac{\Gamma}{2\pi} \int_{-\infty}^{\infty} d\omega \frac{S_s(\mathbf{p}, \omega)}{(E - E_0 - \hbar\omega)^2 + \frac{1}{4}\Gamma^2},$$

where Γ is the total resonance width, E_0 is the resonance energy and $S_s(\mathbf{p},\omega)$ is the self-part of the dynamic structure factor for the isotope to which the resonance belongs. In the case of absorption reactions (i.e. fission, capture) the incident neutron energy, E, is directly related to the momentum transfer component of the dynamic structure factor,

$$|\mathbf{p}| = \sqrt{2mE}$$

where m is the neutron mass. Typically these resonances include temperature effects assuming that the free-gas treatment for the target atom is valid; however, the impact of solid state effects on motion may be included by a calculation of $S_s(\mathbf{p},\omega)$. One such method to include these solid states effect is the phonon expansion method, which assumes the harmonic approximation and uses the partial phonon density states to calculate the self-part the dynamic structure.

The LEAPR module of the NJOY99 code was used to calculate the symmetric form of S(α,β) in ENDF-VI format. A C++ routine was developed to extract this S(α,β) in the full form to perform the broadening integral shown above.

Milestone Status Table:

The milestone status table is given in the project record at www.neup.gov .

Budget Data (1/7/2015):

Budget data are given in the project record at www.neup.gov .